CrossMark

Simple route for preparation cobalt tungstate nanoparticles with different amino acids and its photocatalyst application

Mohammad Vosoughifar[1]

Abstract Nanoparticles sphere-like cobalt tungstate ($CoWO_4$) have been successfully synthesized via the co-precipitation method process by using cobalt (II) nitrate hexahydrate and $Na_2WO_4 \cdot 2H_2O$. Capping agents are frequently used in colloidal synthesis to inhibit nanoparticle overgrowth and aggregation as well as to control the structural characteristics of the resulted nanoparticles in a precise manner; therefore, valine, glycine, and alanine were applied as capping agents. Besides, the effect of valine, glycine, and alanine on the morphology and size of final products were investigated by SEM analysis. According to the vibrating sample magnetometer, cobalt tungstate nanoparticles indicated a paramagnetic behavior at room temperature. The morphology and particle size of products were investigated by SEM images, XRD patterns, UV–Vis and EDS spectroscopy. The photocatalytic characteristics of as-obtained nanocrystalline cobalt tungstate were also examined by degradation of methyl orange (MeO) dye as water contaminant.

1 Introduction

Semiconductors have many highly structurally sensitive properties that are necessary for technological applications like photocatalytic activity. The basis of searching for effective photocatalysts is the understanding of the nature of photocatalysis and its relevant influencing factors. It is documented that the activity of a photocatalystis closely related to surface area, morphology, crystal structure, and electronic Structure as well. The surface are and morphology can be taken as external factors since they can be well controlled by experimental conditions, while crystal electronic structure are intrinsic nature of the photocatalytic activities [1–11]. Recently, a remarkable attentions have been given on application wolframite-type tungstates of transition metals (MWO_4; A = Mn, Fe, Cu, Ni, Pb, Zn, earth rare elements) for photocatalytic degradation of organic compounds [12–14]. These materials are used as photocatalyst, photoluminescence, photovoltaic, super capacitors, conventional oxidation catalysts, magnetic materials multiferroics, molecular precursors to metal tungstates, optical ibers, scintillators, and etc. The previous investigations have shown that the tungsten oxide (WO_3) is an active photocatalyst material for oxygen evolution, while it does not hydrogen evolution neither. Therefore, various eforts have been performed to obtain a series of materials based on AWO_3 and AWO_4 as power full photocatalyst compounds. In this way the resulted materials exhibited interesting technological properties such as ionic photoluminescence, ferro elasticity and conductivity [15–18]. However, the synthesize of AWO_4 may carried out by various methods such as sol–gel, solution combustion synthesis, solid-state reaction, co-precipitation, and solvothermal and hydrothermal synthesis [19–21]. It seems that the co-precipitation method includes various advantageous such as economic, simple, faster, soft chemical synthetic methodology, needs to low calcination temperature, and does not require special working conditions [22]. Hence, in this manuscript, a simple precipitation method was performed to synthesize and characterize of $CoWO_4$ nanoparticles in distilled water as solvent. In addition, the effects of different capping agents such as valine, glycine, and alanine were investigated as capping agents on the morphology and particle size of cobalt tungstate

✉ Mohammad Vosoughifar
mohammadvosoughifar655@gmail.com

1 Young Researchers and Elite Club, Central Tehran Branch, Islamic Azad University, Tehran, Iran

nanostructures. Moreover, the photocatalytic degradation was investigated using methyl orange (MO) under ultraviolet light irradiation to study the photocatalytic activity of as-prepared nanoparticles.

2 Experimental

2.1 Characterization

All the chemicals used in this method were of analytical grade and used as-received without any further purification. X-ray diffraction (XRD) patterns were recorded by a Philips-X'PertPro, X-ray diffractometer using Ni-filtered Cu Kα radiation at scan range of $10 < 2\theta < 80$. Scanning electron microscopy (SEM) images were obtained on LEO-1455VP equipped with an energy dispersive X-ray spectroscopy. Spectroscopy analysis (UV–Vis) was carried out using shimadzu UV–Vis scanning UV–Vis diffuse reflectance spectrometer. The energy dispersive spectrometry (EDS) analysis was studied by XL30, Philips microscope. The magnetic measurement of samples were carried out in a vibrating sample magnetometer (VSM) (Meghnatis Daghigh Kavir Co.; Kashan Kavir; Iran) at room temperature in an applied magnetic field sweeping between $\pm 10,000$ Oe.

2.2 Synthesis of CoWO$_4$ nanoparticles

CoWO$_4$ nanoparticles were prepared by simple coprecipitation method. In a typical procedure, an aqueous solution of cobalt (II) nitrate hexahydrate in the presence of different capping agent, such as valine, glycine, and alanine was mixed with sodium tungstate dihydrate (Na$_2$WO$_4$·2H$_2$O) aqueous solution and the solution was heated up to 70 °C for 15 min. The green precipitate was centrifuged, washed out with distilled water and methanol for three times and dried under vacuum at 60 °C and then calcined at 500 °C for 120 min in a conventional furnace in air atmosphere. Reaction conditions are listed in Table 1 (Fig. 1).

2.3 Photocatalytic experimental

The photo-degradation of methyl orange (MO) in water solutions under ultraviolet light was evaluated to access the photocatalytic activity of CoWO$_4$ nanoparticles. The experiments were performed using a 50 mL solution of methyl orange also containing 0.1 g of CoWO$_4$ nanoparticles after 30 min of aeration. The solution was next transferred to a photo-reactor. The reaction vessel was placed 15 cm away from the 400 W ultraviolet source (mercury lamps) and was kept at ambient temperature. Both before the onset of the reaction and at 10 min intervals of its beginning aliquots

Table 1 The preparation conditions of the CoWO$_4$ nanoparticles

Sample no.	Capping agents	Solvent	Temperature °C	Decolorization(%)
1	Valine	Water	500	82
2	Glycine	Water	500	–
3	Alanine	Water	500	–

of the mixture were taken and their MO contents were determined through UV–Vis spectrometry. Based on the obtained data the degradation percentages of MO were calculated using the below equation:

$$\text{Degradation rate } (\%) = \frac{A_0 - A}{A_0} \times 100 \quad (1)$$

In which A_0 and A represent the absorbance of the solution before the onset of the reaction and at each interval.

3 Results and discussion

In the third millennium, current studies show that different type of surfactants such as ionic, polymeric; etc play a fundamental role in synthesis procedures [23–34]. Moreover, polymeric surfactants are essential materials for preparation of many disperse systems such as solid/liquid dispersions (usually referred to as suspensions); therefore, in this research we examined the effect of capping agents such as valine, glycine, and alanine on the morphology and particle size of final products. Figure 2a–c shows the SEM images of the sample 1–3, respectively. According to the Fig. 2 a, b, product mainly consists of spherical shape nanoparticles with average particle size 50–80 nm. Furthermore, in the presence of valine and glycine as capping agent products have smaller size than alanine as the capping agent.

The powder X-ray difraction technique was used to evaluation of crystal structure and phase purity of CoWO$_4$ nanoparticles and the data has been shown in Fig. 2. The XRD peaks demonstrated a well match with the pure monoclinic phase of CoWO$_4$ nanoparticles with space group of P2/a and JCPDS no. 15–0867. Also no additional peaks were observed because of purity of samples. By the Debye–Scherrer approximation the crystallite size of CoWO$_4$ nanoparticles were calculated from XRD data as 14 nm.

$$D_c = K\lambda/\beta\cos\theta \quad \text{Scherer equation}$$

where β is the breadth of the observed diffraction line at its half intensity maximum, K is the so-called shape factor, which usually takes a value of about 0.9, and λ is the wavelength of X-ray source used in XRD. The morphology
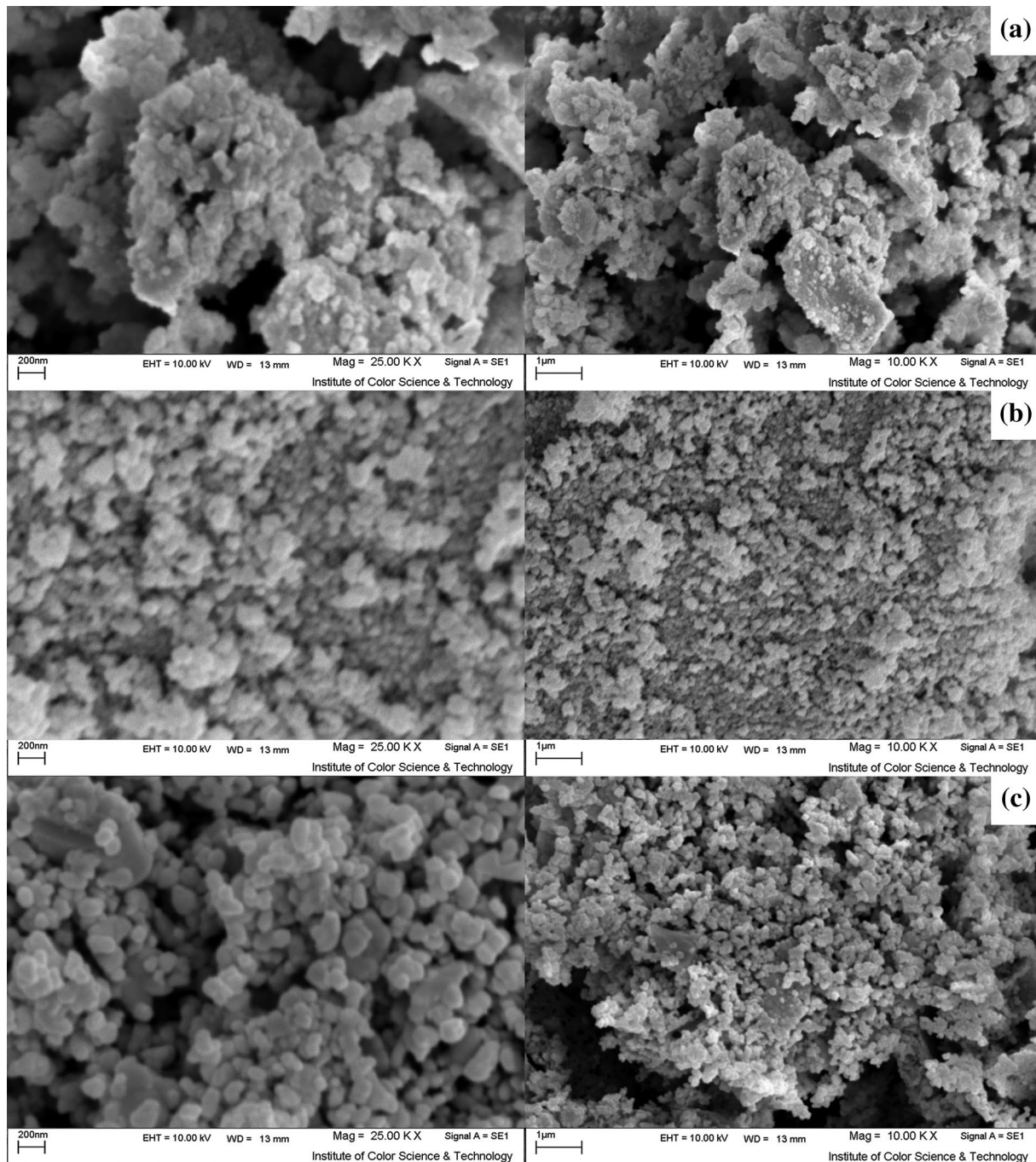
Fig. 1 SEM image of $CoWO_4$ nanoparticles calcined at 500 °C **a** sample 1, **b** sample 2 and **c** sample 3

and shape of $CoWO_4$ nanoparticles were investigated by SEM method and the results conirmed that the particles are packed with an average size of 50–80 nm (See Fig. 1a–c). Also the results demonstrated that the particle size that obtained by SEM is larger than obtained by XRD because of the SEM shows the sum of many crystallites. The purity of nanocrystalline product was also confirmed by EDS analysis (Fig. 3). According to Fig. 3, the sample

no. 1 is composed of Co, W and O elements. Furthermore, no impurity peaks are seen, which indicates a high level of purity in the sample. The VSM magnetic measurements for the cobalt tungstate oxide (Fig. 4) show the magnetic properties of nanoparticles calcined at 500 °C. The $CoWO_4$ nanoparticles exhibit paramagnetic behaviour at room temperature, with a saturation magnetization of 0.13 emu/g. Figure 5 shows the $(\alpha h\upsilon)^2$ vs hy curve of $CoWO_4$

Fig. 2 XRD pattern of CoWO$_4$ nanoparticles calcined at 500 °C (sample 1)

Fig. 3 EDS pattern of CoWO$_4$ nanoparticles calcined at 500 °C (sample 1)

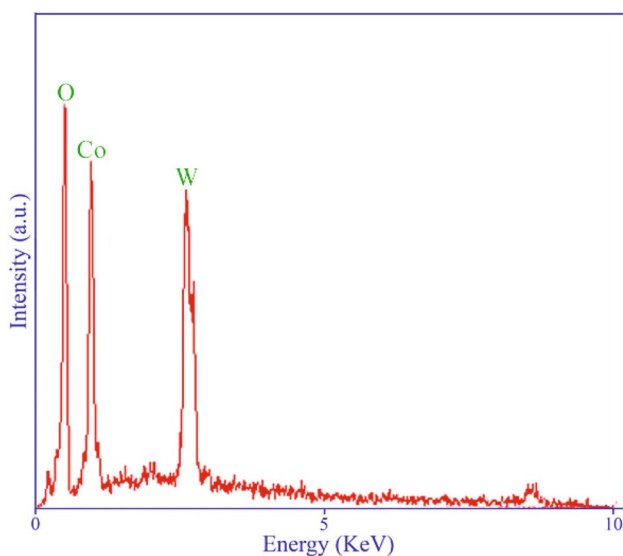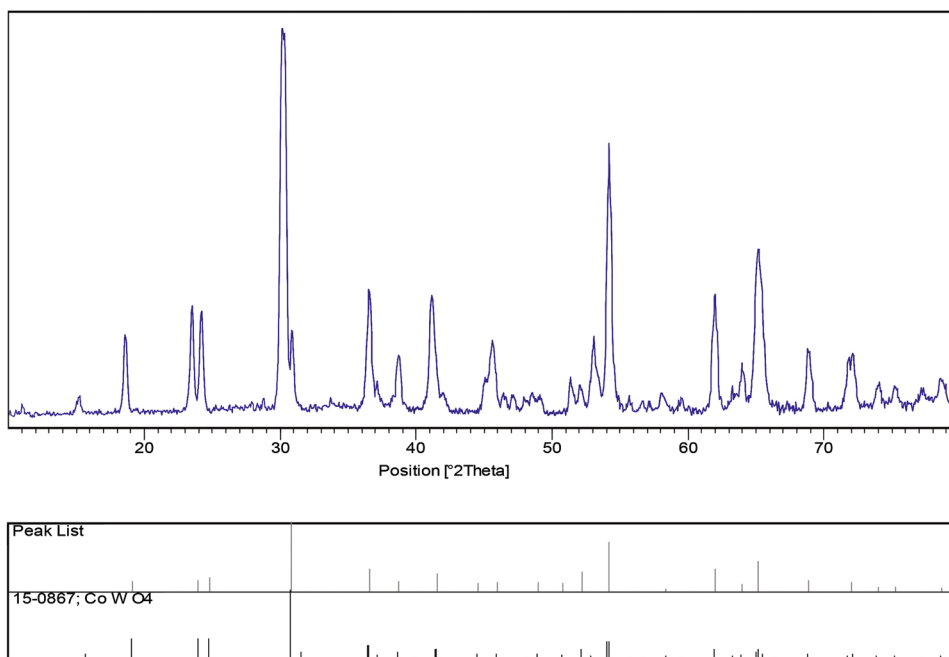**Fig. 4** VSM curves of CoWO$_4$ nanoparticles calcined at 500 °C (sample 1)

nanoparticles which were calculated from their UV–Vis absorbance using the equation proposed by Wood and Tauc exhibited the equation below.

$$\alpha h\upsilon = (h\nu - Eg)^n \tag{2}$$

where a is the absorbance, h the Planck constant, y the photon frequency, Eg the energy gap, and n the pure numbers associated with the different types of electronic transitions. For n = 1/2, 2, 3/2 and 3, the transitions are directly allowed, indirectly allowed, directly forbidden,
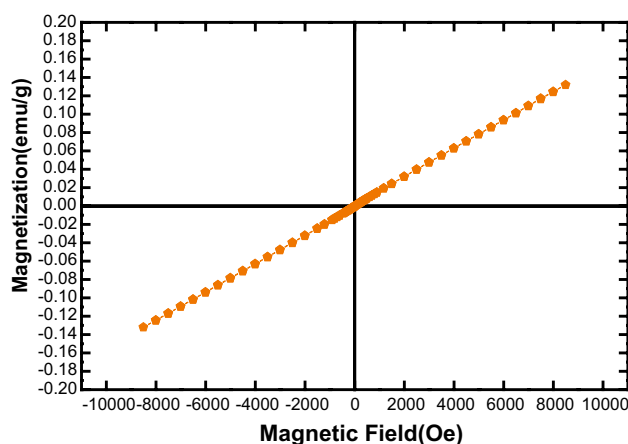
and indirectly forbidden, respectively. Each energy gap was determined by extrapolation of each linear portion of the curves to a = 0. In the present research, the CoWO$_4$ presents directly allowed electronic transition (n = 1/2) and the energy gaps of CoWO$_4$ nanoparticles is 3.1 eV. Photodegradation of methyl orange (MO) as water contaminant under UV light illumination was employed to evaluate the properties of the as-synthesized CoWO$_4$ nanoparticles. Figure 6 exhibits the obtained result. No methyl orange was practically broken down after 70 min without employing UV light illumination or as-prepared nanoparticles CoWO$_4$. This observation illustrated that the contribution of self-degradation was insignificant. The proposed mechanism of
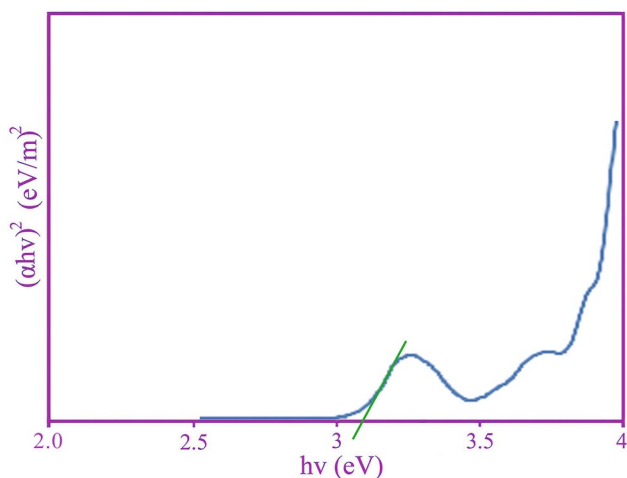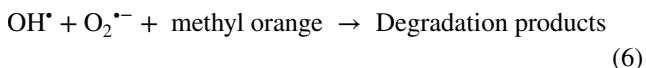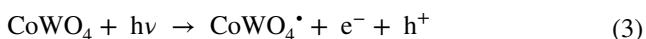
Fig. 5 DRS pattern of $CoWO_4$ nanoparticles calcined at 500 °C (sample 1)

CoWO$_4$ nanoparticles have high potential to be applied as favorable and appropriate material for photocatalytic applications under illumination of UV light. The heterogeneous photocatalytic processes have diffusion, adsorption and reaction steps. It has been shown that the desirable distribution of the pore has effective and important impact on the diffusion of the reactants and products, and therefore effects on the photocatalytic activity. It seems that the enhanced photocatalytic activity of the as-obtained nanoparticles CoWO$_4$ can be owing to desirable and appropriate distribution of the pore, high hydroxyl amount and high separation rate of charge carriers (Scheme 1). Furthermore, this route is facile to operate and very suitable for industrial production of CoWO$_4$ nanoparticles [35–42].

the photocatalytic degradation of the methyl orange can be assumed as:

$$CoWO_4 + h\nu \rightarrow CoWO_4^{\bullet} + e^- + h^+ \tag{3}$$

$$h^+ + H_2O \rightarrow OH^{\bullet} \tag{4}$$

$$e^- + O_2 \rightarrow O_2^{\bullet-} \tag{5}$$

$$OH^{\bullet} + O_2^{\bullet-} + \text{methyl orange} \rightarrow \text{Degradation products} \tag{6}$$

Utilizing photocatalytic calculation by Eq. (1), the methyl orange degradation was about 82% after 70 min illumination of UV light in the presence of samples 1. This obtained result demonstrates that as-prepared

4 Conclusions

A strong photocatalyst CoWO$_4$ nanoparticles was synthesized by a co-precipitation method. Several amino acid such as valine, glycine, and alanine were used as capping agent in order to obtained various morphology and size of CoWO$_4$ nanoparticles. The VSM results demonstrated that all type of CoWO$_4$ nanoparticles has a remarkable paramagnetic property. Also, the MO degradation by employing of photocatalytic effect of CoWO$_4$ nanoparticles was about 81% after 80 min irradiation of UV light. The results indicated that the CoWO$_4$ nanoparticles are interesting materials for photocatalytic applications under UV light to degradations of organic materials.

Fig. 6 Photocatalytic methyl orange degradation of CoWO$_4$ nanoparticles under ultraviolet light
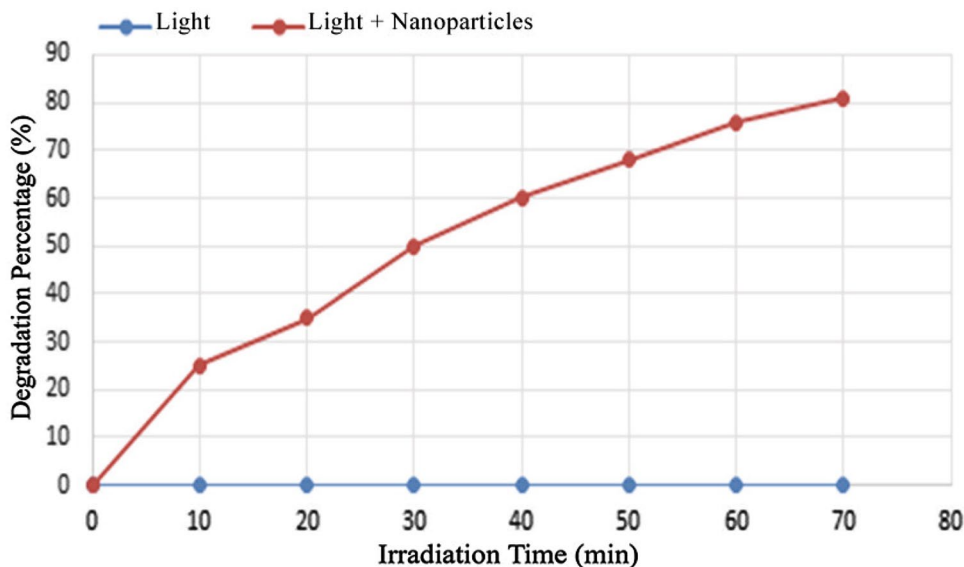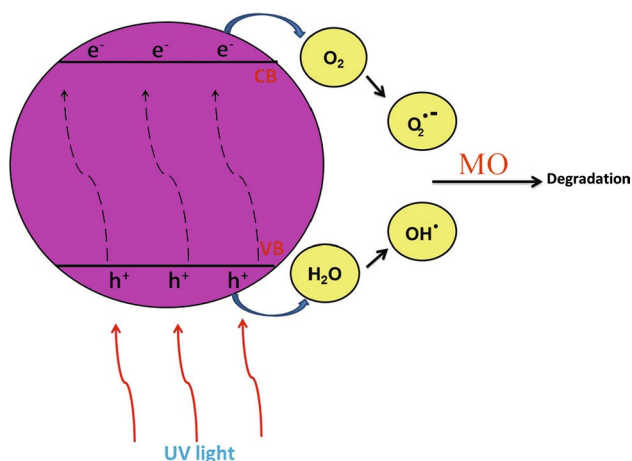
Scheme 1 Reaction mechanism of methyl orange photodegradation over $CoWO_4$ nanoparticles under UV light irradiation

References

1. F. Azizi, F. molani J. Nanostruct. 6, 58 (2016)
2. S. Farhadi, F. Siadatnasab, K. Jahanara, J. Nanostruct. 3, 227 (2013)
3. S. Khademolhoseini, J. Mater. Sci. 27, 10759 (2016)
4. R. Talebi, J. Mater. Sci. 27, 3565 (2016)
5. A. S. M. Hosseinpour-mashkani, A. Sobhani-Nasab, J. Mater. Sci. 27, 7548 (2016)
6. A. Sobhani-Nasab, M. Behpour, J. Mater. Sci. 27, 11946 (2016)
7. M. Rahimi-Nasrabadi, M. Behpour, A. Sobhani-Nasab, M.R. Jeddy, J. Mater. Sci. 27, 11691 (2016)
8. S.A. Hosseini, J. Mater. Sci. 27, 6517 (2016)
9. R. Talebi, J. Mater. Sci. 27, 10770 (2016)
10. M. Behpour, M. Mehrzad, S.M. Hosseinpour-Mashkani, J. Nanostruct. 5, 183 (2015)
11. M. Salavati-Niasari, F. Soofivand, A. Sobhani-Nasab, M. Shakouri-Arani, A. Yeganeh Faal, S. Bagheri, Adv. Powder Technol. 27, 2066 (2016)
12. U.M. Garca-Perez, A. Martnez-de la Cruz, J. Peral, Electrochim. Acta 81, 227 (2012)
13. J. Ungelenk, M. Speldrich, R. Dronskowski, C. Feldmann, Solid State Sci. 31, 62 (2014)
14. K.V. Dabre, S.J. Dhoble, J. Lochab, J. Lumin. 149, 348 (2014)
15. M. Rahimi-Nasrabadi, S.M. Pourmortazavi, M.R. Ganjali, A.R. Banan, F. Ahmadi, J. Mol. Struct. 1074, 85 (2014)
16. K. Adib, M. Rahimi-Nasrabadi, Z. Rezvani, S.M. Pourmortazavi, F. Ahmadi, H.R. Naderi, M.R. Ganjali, J. Mater. Sci. Mater. Electron. 27, 4541 (2016).
17. Y.X. Zhou, H.B. Yao, Q. Zhang, J.Y. Gong, S.H. Liu, S.J. Yu, Inorg. Chem 48, 1082 (2009)
18. J.M. Quintana-Melgoza, A. Gmez-Cortés, M. Avalos-Borja, React. Kinet. Catal. 76, 131 (2002).
19. M. Bonanni, L. Spanhel, M. Lerch, E. Fuglein, G. Muller, F. Jermann, Chem. Mater. 10, 304 (1998)
20. A.R. Phani, M. Passacantando, L. Lozzi, S. Santucci, J. Mater. Sci. 35, 4879 (2000)
21. F.S. Wen, X. Zhao, H. Huo, J.S. Chen, E. Shu Lin, J.H. Zhang, Mater. Lett. 55, 152 (2002)
22. S.M. Pourmortazavi, M. Rahimi-Nasrabadi, Y. Fazli, M. Mohammad Zadeh, Appl. Phys. A. 119, 929 (2015)
23. A. Sobhani-Nasab, M. Rangraz-Jeddy, A. Avanes, M. Salavati-Niasari, J. Mater. Sci. 26, 9552 (2015)
24. A. Sobhani-Nasab, M. Behpour, J. Mater. Sci. 27, 1191 (2016)
25. A. Sobhani-Nasab, S.M. Hosseinpour-Mashkani, M. Salavati-Niasari, S. Bagheri, J. Clust. Sci. 26, 1305 (2015)
26. A. Sobhani-Nasab, S.M. Hosseinpour-Mashkani, M. Salavati-Niasari, H. Taqriri, S. Bagheri, K. Saberyan, J. Mater. Sci. 26, 5735 (2015)
27. S.M. Hosseinpour-Mashkani, M. Maddahfar, A. Sobhani-Nasab, J. Mater. Sci. 27, 474 (2016)
28. M. Behpour, M. Chakeri, J. Nanostruct. 2, 227 (2012)
29. S.M. Hosseinpour-Mashkani, A. Sobhani-Nasab, M. Maddahf, J. Nanostruct. 6, 67 (2016)
30. S.S. Hosseinpour-Mashkani, S.S. Hosseinpour-Mashkani, A. Sobhani-Nasab, J. Mater. Sci. 27, 4351 (2016)
31. A. Sobhani-Nasab, M. Sadeghi, J. Mater. Sci. 27, 7933 (2016)
32. M. Ramezani, A. Sobhani-Nasab, A. Davoodi, J. Mater. Sci. 26, 5440 (2015)
33. S.M. Hosseinpour-Mashkani, M. Maddahfar, A. Sobhani-Nasab, J. Electron Mater. 45, 3612 (2016)
34. S.M. Hosseinpour-Mashkani, A. Sobhani-Nasab, J. Mater. Sci. 27, 3240 (2016)
35. S.M. Hosseinpour-mashkani, A. Sobhani-Nasab, M. Mehrzad, J. Mater. Sci. 27, 5758 (2016)
36. M. Aliahmad, A. Rahdar, Y. Azizi, J. Nanostruct. 4, 145 (2014)
37. M. Enhessari, M. Kargar-Razi, P. Moarefi, A. Parviz, J. Nanostruct. 2, 119 (2012)
38. L. Torkian, E. Amereh, J. Nanostruct. 6, 307 (2016)
39. M. Ebadi, H. Shagholani, H. Jahangir, J. Nanostruct. 6, 23 (2016)
40. A. Kabiri, G. Nabiyouni, P. Boroujerdian, J. Ghasemi, A. Fattahi, J. Nanostruct. 3, 421 (2013)
41. M.R. Dousti, R.J. Amjad, J. Nanostruct. 3, 435 (2013)
42. L. Hashemi, A. Tahmasian, A. Morsali, J. Abedini, J. Nanostruct. 2, 163 (2012)